IOPscience iopscience.iop.org

Home Search Collections Journals About Contact us My IOPscience

Evolution of optical constants and electronic structure of disordered $Si_{1-x}Ge_x$ alloys

This article has been downloaded from IOPscience. Please scroll down to see the full text article.

2001 J. Phys.: Condens. Matter 13 777

(http://iopscience.iop.org/0953-8984/13/4/323)

View the table of contents for this issue, or go to the journal homepage for more

Download details:
IP Address: 171.66.16.226
The article was downloaded on 16/05/2010 at 08:25

Please note that terms and conditions apply.

INSTITUTE OF PHYSICS PUBLISHING JOURNAL OF PHYSICS: CONDENSED MATTER

J. Phys.: Condens. Matter **13** (2001) 777–786 www.iop.org/Journals/cm PII: S0953-8984(01)16558-6

Evolution of optical constants and electronic structure of disordered $Si_{1-x}Ge_x$ alloys

Jae Ho Bahng[1], **K J Kim**[2], **S H Ihm**[3], **J Y Kim**[3] **and H L Park**[1]

[1] Department of Physics and IPAP, Yonsei University, Seoul 120-749, Korea
[2] Department of Physics, Konkuk University, Seoul 143-701, Korea
[3] Department of Physics and Semiconductor Physics Research Center, Jeonbuk National University, Jeonju 560-756, Korea

Received 21 August 2000

Abstract

The energy shifts of optical interband transition edges, $E_0^{'}$, E_1, $E_1+\Delta_1$ and E_2, of relaxed $Si_{1-x}Ge_x$ alloys grown epitaxially on Si(001) substrates by molecular beam epitaxy have been studied as a function of Ge composition using their complex dielectric functions measured by spectroscopic ellipsometry at room temperature. The interband transition edges were resolved by a line shape fitting on the numerical second derivative spectra of the dielectric functions. The $E_0^{'}$, E_1, $E_1+\Delta_1$ and $E_2(\Sigma)$ edges are found to shift to lower energies with increasing Ge composition while the $E_2(X)$ edge shifts to higher energies. Also it is found for E_1 and $E_1+\Delta_1$ energies that downward bowing exists and for Δ_1 energy that upward bowing exists. These behaviours of the transition edges are understood by comparing the band structure of Si with that of Ge and interpreted as due to the effect of the random potential originated by alloying disorder.

1. Introduction

Si and Ge are miscible in all proportions, forming a solid solution of $Si_{1-x}Ge_x$ over the entire composition. The lattice constants of unstrained $Si_{1-x}Ge_x$ alloys have been measured and Vegard's law is found to be a good approximation [1]. Such binary alloys $Si_{1-x}Ge_x$ have been extensively studied due to the possibility [2] for electronic device applications such as heterojunction bipolar transistors [2], modulation-doped field-effect transistors [3], and quantum-well infrared sensors [4]. Research about the optical properties and related optical transitions of this alloy system has been widely performed because it can give valuable information for understanding the electronic band structures and determining critical band parameters useful for its technological applications [5].

Kline *et al* [6] have shown that the linear dependences between the transition energies of Si and those of Ge exist as a function of Ge composition for relaxed $Si_{1-x}Ge_x$ alloys. Humlicek *et al* [7] reported dielectric functions of relaxed-grown $Si_{1-x}Ge_x$ alloys measured by spectroscopic ellipsometry (SE) for the entire Ge composition and a quadratic dependence of E_1 interband transition energy as a function of the Ge composition. Thereafter, a number of

 © 2001 IOP Publishing Ltd Printed in the UK

SE studies have been performed on relaxed and strained $Si_{1-x}Ge_x$ epitaxial films [8–11]. But these studies are restricted to small ranges (x < 0.3) of Ge composition. Therefore, for all Ge compositions, to know the energy shifts of the $E_0^{'}$, E_1, $E_1+\Delta_1$, and E_2 edges as a function of Ge composition is considered to be important because it can give critical information on how the electronic band structure of the alloy system evolves and provide the band parameters for device applications.

In this work, the dielectric functions of $Si_{1-x}Ge_x$ alloy films grown by molecular beam epitaxy (MBE) on Si(001) substrates were measured by SE and compared with those of Si and Ge. For such an investigation, complex dielectric functions, $\epsilon = \epsilon_1 + i\epsilon_2$, for a number of relaxed $Si_{1-x}Ge_x$ alloys for all compositions ($0.0 \leqslant x \leqslant 1.0$) were measured by SE in the 2–6 eV photon energy ranges at room temperature. The composition dependence of the characteristic critical-point energies of the alloys was quantitatively estimated using a line shape analysis on the second derivative spectra of dielectric functions. The variation in the critical-point energies as a function of Ge composition can provide information about the evolution of the band structure of the alloy system.

2. Experimental details

$Si_{1-x}Ge_x$ alloy films with Ge compositions of 0.07, 0.15, 0.2, 0.4, 0.6 and 0.8 were used in the present optical study. They were grown by MBE on Si(001) at a substrate temperature of 730 °C. Their thicknesses were set to be about 1 μm in order to remove the effect of lattice-mismatch-induced strain within the penetration depth of the incident photon beam. The average Ge composition throughout the epilayer was controlled by the ratio of Si and Ge flux and the epilayer thickness was controlled by the growth time. Also, they were estimated by double-crystal x-ray diffraction measurement. For comparison with the alloys, (100)-oriented Si and Ge wafers were used.

SE measurements were performed on the samples at room temperature with a rotating-analyzer ellipsometer [12] in the 2–6 eV photon energy region with an energy interval of 0.01 eV. The continuum light source was a high-pressure 75 W Xe short-arc lamp with a range of 1.5–6.5 eV. An ARC SpectraPro-275 monochromator with a 1200 groove/nm grating was used to produce quasi-monochromatic light with a spectral resolution of 0.1 nm for 435.8 nm and a focal length of 0.275 m. Then the light through the monochromator was focused by a spherical mirror with 0.3 m focal length. We used crystal quartz Rochon prisms that were constructed by optically contacting the prism halves [12] for the polarizer and analyser prism, respectively. Also, in order to reduce the instability of rotating speed, we used a stepping motor with 400 step/360° for the rotating analyser. For the fixed polarizer, we used the Model 20010 motor of Oriel Co. which rotates in 0.01° steps in order to perform an accurate calibration. For our detector, we used an ARC R928 side-on photomultiplier tube with a range of 1.5–6.5 eV.

From the result of the SE measurement, the complex dielectric function can be obtained by a two-phase model (air and sample) [13] and represented by

$$\epsilon = \sin^2\phi + \sin^2\phi\tan^2\phi\frac{(1-\rho)^2}{(1+\rho)^2} \tag{1}$$

where ρ is the complex reflectance ratio ($= r_p/r_s$) of the p (parallel) and s (perpendicular) field components of the light beam defined with respect to the plane of incidence of the sample obtained by SE measurement and ϕ is an angle of incidence, 70.5° in the present measurements. The epilayer thicknesses of the samples are sufficiently greater than the effective penetration depth, δ [14], of the light beam in the absorption region of their dielectric functions, where δ can be qualitatively estimated to be $\delta = \lambda/4\pi\kappa$, with λ being the wavelength of the light beam

and κ the imaginary part of the complex refractive index, related to the complex dielectric function by $\epsilon^{1/2} = n + i\kappa$.

All the samples were chemically etched in a solution of 8:4:1, HNO_3:H_2O:HF at room temperature for about 1 minute before the SE measurements in order to reduce the effect of the surface oxide layer [15].

3. Results and discussion

Real (ϵ_1) and imaginary (ϵ_2) parts of the measured dielectric functions of the relaxed $Si_{1-x}Ge_x$ alloys with Ge compositions of 0.2, 0.4, 0.6 and 0.8 are exhibited and compared with those of pure Si and Ge in figures 1(a) and (b), respectively. It is seen in figure 1(b) that two strong absorption structures exist for the Si sample at about 3.4 and 4.2 eV. These absorption structures are known to originate from direct band-to-band transitions at various regions in the Brillouin zone (BZ) of Si. The 3.4 eV structure is known to be due to the E_0', E_1 and E_1+Δ_1 interband transition edges and the 4.2 eV structure due to $E_2(X)$ and $E_2(\Sigma)$ edges [5, 16]. The sharpness of the 3.4 eV structure indicates that the three edges are located close to each other in energy. The band structure of Ge differs from that of Si most significantly in the conduction band arrangement. For example, the Γ_{15}^c and $\Gamma_{2'}^c$ levels reverse their ordering. Moreover, while Ge and Si are both indirect semiconductors, the conduction band minimum in Ge occurs at the L-point as opposed to a point near X in Si.

For the Ge sample, it is seen in figure 1(b) that there are three structures at about 2.2, 3.3 and 4.2 eV. From the band structure of Ge [5], the 2.2 eV structure is interpreted as due to the E_1 and E_1+Δ_1 interband transition edges, the 3.3 eV structure due to the E_0' edge, and the 4.2 eV structure due to the E_2 edge. The E_1 and E_1+Δ_1 edges of Ge are significantly shifted to lower energies compared with the transition edges of Si, while the E_0' and E_2 edges are scarcely shifted.

From the evolution of the dielectric function spectra in figure 1, it is seen that the structure due to the E_1 edge of the $Si_{1-x}Ge_x$ alloys shifts gradually to lower energies as the Ge composition increases, while the structure due to the E_0' edge remains at about same energy. For E_2 edges, we have found that the structure due to E_2 edges of $Si_{1-x}Ge_x$ alloys is hardly shifted from that of Si and Ge, but its intensity is reduced from that of Si to that of Ge as the Ge composition increases. It is interpreted as due to the effect of the alloying of Si and Ge. Also, a decrease of the height of the ϵ_1 and ϵ_2 values at the structure due to the E_1 edge occurs up to concentrations of $x \sim 0.6$, then this feature begins to reemerge smoothly until it reaches the corresponding value of Ge which is interpreted as due to the alloying disorder.

To know the energies of the E_0', E_1, E_1+Δ_1 and E_2 transition edges in the $Si_{1-x}Ge_x$ alloys is considered to be important because it can give critical information on how the electronic band structure of the alloy system evolves. So, a critical point line shape analysis has been performed for an exact evaluation of the energy shifts of the various transition edges with respect to the Ge composition variation. In order to enhance the structures in figure 1(b), the second derivative spectra of the dielectric functions, $d^2\epsilon/dE^2$, were calculated numerically. An appropriate level of smoothing was also performed in order to remove the noise in the derivative spectra without distorting the line shape. The derivative spectra were fitted to the standard critical point line shapes [16] represented by

$$\frac{d^2\epsilon}{dE^2} = -n(n-1)Ae^{i\phi}(E - E_c + i\Gamma)^{n-2} \qquad n \neq 0 \tag{2}$$

$$Ae^{i\phi}(E - E_c + i\Gamma)^{-2} \qquad n = 0 \tag{3}$$

where A is the amplitude, E_c the critical-point energy, Γ the broadening factor and ϕ the excitonic phase angle. The exponent n has the values of $\frac{-1}{2}$, 0, $\frac{1}{2}$ and -1 for the one-, two-,

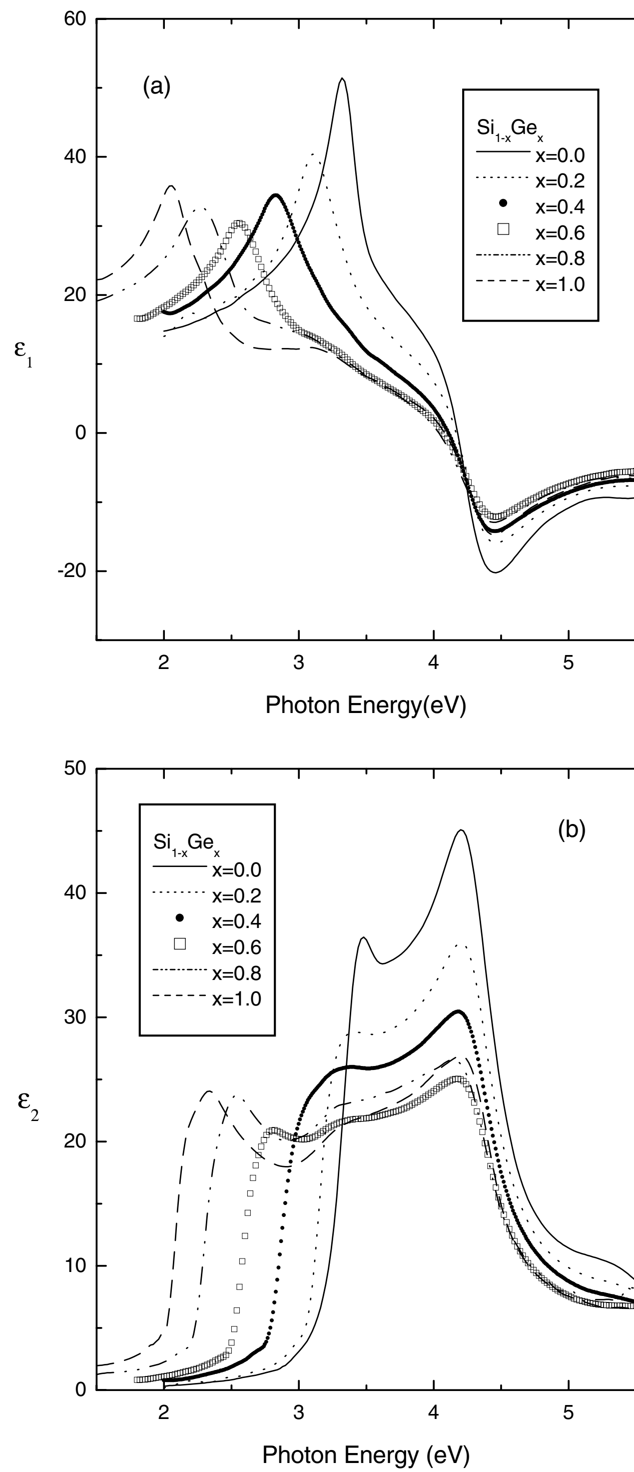

Figure 1. Real (a) and imaginary (b) parts of the dielectric functions of relaxed $Si_{1-x}Ge_x$ alloys with the composition x indicated in the legend.

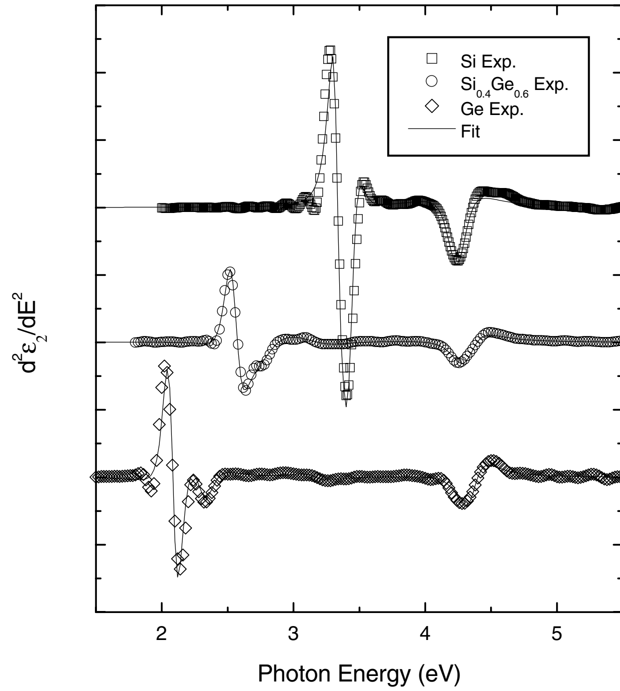

Figure 2. Fits to the second derivatives of the imaginary parts of the dielectric functions of relaxed $Si_{1-x}Ge_x$.

three-dimensional, and excitonic critical points, respectively. A least-squares fitting procedure using the Marquardt algorithm [17] was used for the fit. In the present line shape analysis, the excitonic line shape was assumed for the E_1 and $E_1+\Delta_1$ edges and the two-dimensional line shape for the $E_0^{'}$ and E_2 edges. The excitonic assumption for the E_1 and $E_1+\Delta_1$ edges of the $Si_{1-x}Ge_x$ alloys was found to give an excellent fit quality in discriminating them from the neighbouring $E_0^{'}$ edge. In figure 2, both the second derivative spectra and the fitted curves of Si, $Si_{0.4}Ge_{0.6}$ and Ge are exhibited in order to confirm the fitting quality and a good agreement between them is found. The energies and linewidths of interband transition edges obtained by line shape analysis are listed in table 1.

In the present line shape analysis, the $E_0^{'}$ edge of pure Si was safely resolved from the neighbouring E_1 and $E_1+\Delta_1$ edges. Also, the spin–orbit splitting Δ_1 between the E_1 and

Table 1. Interband transition energies and linewidths (in parentheses) of relaxed $Si_{1-x}Ge_x$ alloy as a function of Ge composition x.

x	E_1 (eV)	$E_1+\Delta_1$ (eV)	$E_0^{'}$ (eV)	$E_2(X)$ (eV)	$E_2(\Sigma)$ (eV)
0	3.398 (0.105)	3.432 (0.108)	3.337 (0.111)	4.259 (0.133)	4.473 (0.158)
0.2	3.075 (0.128)	3.173 (0.139)	3.284 (0.131)	4.266 (0.142)	4.450 (0.161)
0.4	2.850 (0.150)	3.000 (0.170)	3.214 (0.163)	4.269 (0.148)	4.425 (0.177)
0.6	2.555 (0.146)	2.720 (0.165)	3.202 (0.163)	4.280 (0.147)	4.410 (0.175)
0.8	2.295 (0.121)	2.498 (0.155)	3.198 (0.140)	4.274 (0.140)	4.420 (0.170)
1.0	2.09 (0.110)	2.299 (0.140)	3.200 (0.128)	4.298 (0.128)	4.415 (0.144)

$E_1+\Delta_1$ edges of Si was resolved to be 34 meV, which had not been resolved in previous studies [7–11]. Also, the Δ_1 energy of Ge was found to be 0.209 eV in this analysis, which is in good agreement with the result in [18]. The E_1, $E_1+\Delta_1$, $E_0^{'}$ and E_2 energies obtained from the present line shape analysis are exhibited in figure 3 as a function of Ge composition x. The results show a quadratic dependence of the transition energies on Ge concentration. So we have fitted the E_1, $E_1+\Delta_1$, $E_0^{'}$ and E_2 energies using the quadratic equation

$$E(x) = A + Bx + Cx^2 \tag{4}$$

where C is a bowing parameter. The resulting curves are shown in figure 3 by solid lines.

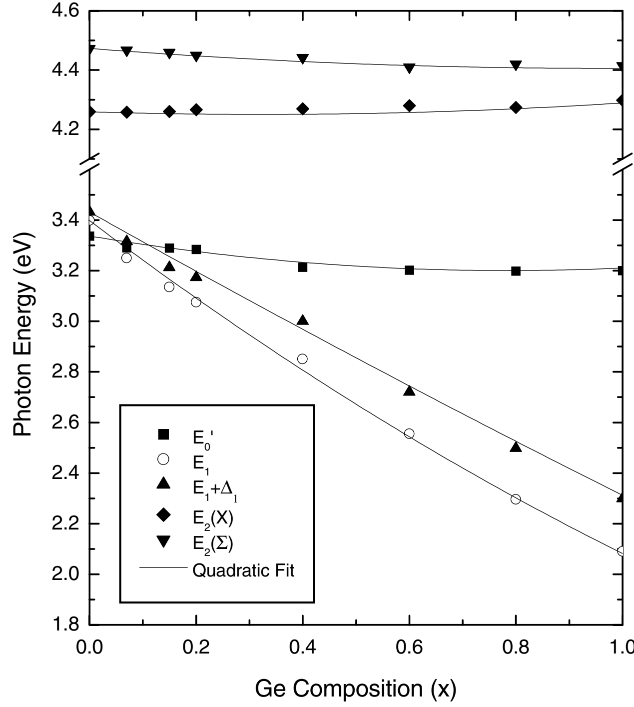

Figure 3. Evolution of $E_0^{'}$, E_1, $E_1+\Delta_1$, $E_2(X)$ and $E_2(\Sigma)$ transition edges for relaxed $Si_{1-x}Ge_x$ alloys with the composition x.

For E_1 and $E_1+\Delta_1$ transition edges, it is found from figure 3 that these transition edges shift to lower energies with a downward bowing and their splitting is increased as the Ge composition increases. The E_1 and its spin–orbit-split $E_1+\Delta_1$ edges are due to the direct interband transitions along the Λ ($\Gamma - L$) direction in the BZ, $\Lambda_{45}^{v} \rightarrow \Lambda_1^{c}$ and $\Lambda_6^{v} \rightarrow \Lambda_1^{c}$, respectively, where the valence and the conduction bands go quite parallel with each other, inducing a strong joint density of states for the transitions. Using equation (4), these curves are represented by the following quadratic equations

$$E_1(x) = 3.398 - 1.586x + 0.27x^2 \tag{5}$$

$$E_1 + \Delta_1(x) = 3.432 - 1.185x + 0.065x^2 \tag{6}$$

respectively. They show downward bowings with positive bowing parameters C and the bowing of the E_1 edge is larger than that of the $E_1+\Delta_1$ edge. These results differ from the results of Kline *et al* [6] in that their transition energies varied linearly with Ge concentration,

but coincide with those of Humlicek *et al* [7] and Pickering *et al* [9] except for the value of the bowing parameter for the E_1 edge. Pickering *et al* [9] reported that the bowing parameter of the E_1 edge was 0.153 eV. The bowing of the fundamental band gap in semiconductor alloys is well known to be mainly caused by the following two contributions [19]. The first contribution to the band gap bowing is the averaged atomic potential in binary alloys and can give either upward or downward bowing. This has been interpreted by the virtual-crystal approximation (VCA) [20, 21], in which the magnitude of the periodic crystal potential varies linearly with alloy composition. The second contribution is the potential fluctuation due to the alloying disorder and known to cause downward bowing mainly. This effect can be explained by the coherent-potential approximation (CPA) [20, 22]. They also can be extended to higher-energy transition edges than the fundamental one. For higher transition edges, the magnitude and the sign of the bowing compared to the fundamental gap can change [23].

The theoretical work on the relaxed $Si_{1-x}Ge_x$ alloy was performed by Krishnamurthy *et al* [20] using both the VCA and CPA. A band structure calculation on relaxed $Si_{1-x}Ge_x$ using VCA showed a linear variation in E_1 energy with x. On the other hand, a band structure calculation using CPA showed that the E_1 energy of the alloys varies with positive bowing. The difference between the VCA and the CPA results [20] was reported to be about 0.08 eV at $x = 0.5$. The present fitting to the experimental results indicates a deviation of the E_1 edge of 0.06 eV at $x = 0.5$ from the linear interpolation between Si and Ge. This indicates that the potential fluctuation due to the alloying disorder mainly affects the downward bowing of the E_1 edge. Also, the bowing parameters are found to be relatively small compared with III–V and II–VI alloys [19, 23–25], which indicates that the disorder effect in $Si_{1-x}Ge_x$ is weaker than that in III–V and II–VI alloys.

A large nonlinearity of Δ_1 is also observed from equations (5) and (6) and is shown in figure 4. Such nonlinearity of Δ_1 also indicates the potential fluctuation in compositionally disordered semiconductor alloys [23]. The variation in the Δ_1 energy as a function of the Ge composition can be fitted by the following quadratic equation

$$\Delta_1(x) = 0.034 + 0.331x - 0.155x^2. \quad (7)$$

This result shows a slight discrepancy with the previous result of $\Delta_1(x) = 0.033 + 0.266x - 0.091x^2$ deduced from the E_1 energy [7] and the $E_1+\Delta_1$ energy [9]. It is mainly due to the downward bowing of the E_1 edge by the alloying disorder. This upward bowing of the Δ_1 is observed in many studies for various semiconductor alloys such as $In_{1-x}Ga_xAs_yP_{1-y}$ [19], $Zn_xCd_{1-x}Se$ [23] and $Al_xGa_{1-x}As$ [24]. Figure 5 shows the Lorentzian broadening parameters Γ for all of the CPs obtained from a line shape analysis. We also have found that the linewidths increase with increasing Ge composition until $x = 0.4$ and then decrease. This fact indicates that the quantity of disorder increases until $x = 0.4$ and then decreases.

The E_0' interband transition is due to the direct interband transitions near the Γ point of the Brillouin zone (BZ) between the $\Gamma^v_{25'}$ valence band and Γ^c_{15} conduction band, i.e. $\Gamma^v_{25'} \rightarrow \Gamma^c_{15}$. It is found that the E_0' transition edge slightly shifts to lower energies with increasing Ge composition and has downward bowing as in the case of the E_1 transition edge. But the dependence of the E_0' transition on the Ge composition is small, that is about 20% of that of the E_1 energy. The Ge composition dependence of the E_0' edge is represented by

$$E_0'(x) = 3.337 - 0.348x + 0.222x^2. \quad (8)$$

This result for the E_0' transition edge differs from Kline *et al*'s result [6] and from that of Humlicek *et al* [7] in the linear dependence on the Ge composition. From figure 3, it is seen that E_1 and E_0' transition edges are crossed at $x \sim 0.05$ and this result is in good agreement with many other experimental results [8–10].

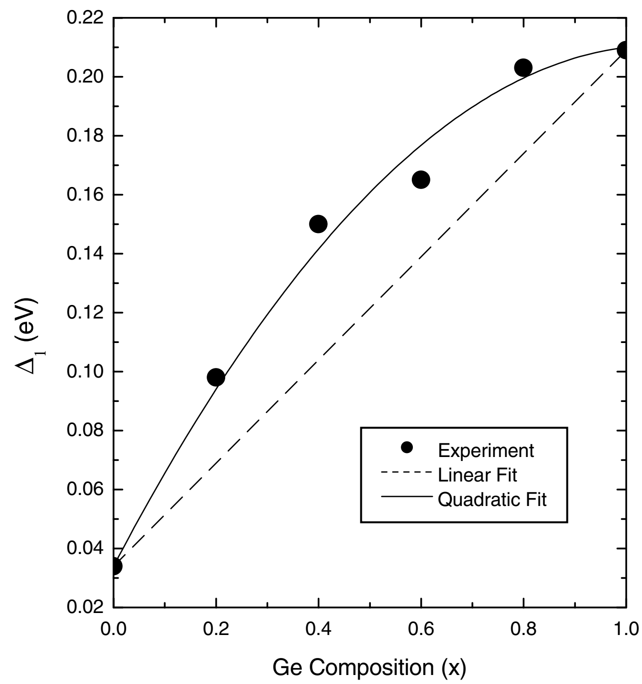

Figure 4. Concentration dependence of spin–orbit splitting band gap Δ_1.

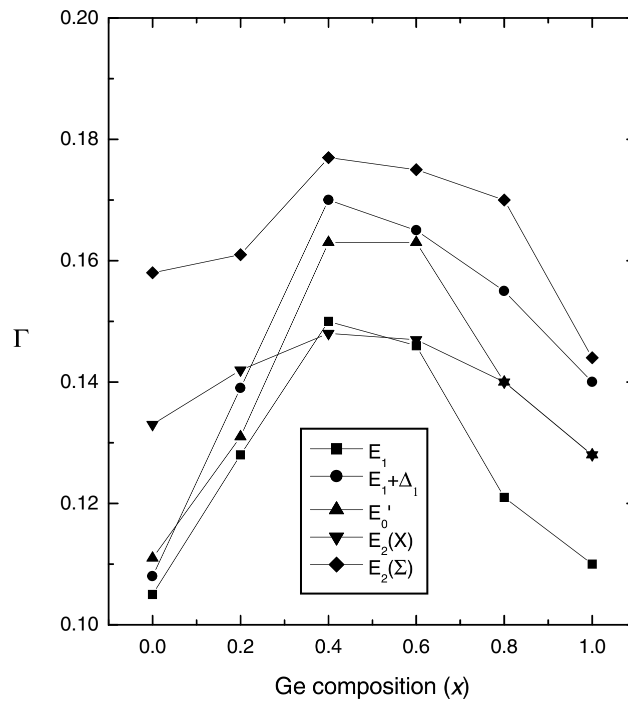

Figure 5. Lorentzian broadening parameters Γ for all of the CPs obtained from the line shape analysis.

The major strength of the 4.2 eV structure comes near the X point and along the Σ $(\Gamma - K)$ directions designated by the E_2 edges [5]. For E_2 transition edges, it is seen in figure 3 that the $E_2(X)$ transition edge shifts to higher energies and the $E_2(\Sigma)$ edge to lower energies as the Ge composition increases so that their energy difference becomes reduced, but these amounts are very small. These curves are

$$E_2(X)(x) = 4.259 - 0.052x + 0.084x^2 \quad (9)$$

$$E_2(\Sigma)(x) = 4.473 - 0.139x + 0.072x^2 \quad (10)$$

respectively. By comparison with our results, the measurement of Carline *et al* [10] for the E_2 transition appears to be a superposition of the transitions $E_2(X)$ and $E_2(\Sigma)$.

4. Summary

Dielectric functions of the relaxed $Si_{1-x}Ge_x$/Si(001) alloys ($0.07 \leqslant x \leqslant 0.8$) grown by MBE, Si and Ge samples have been measured by spectroscopic ellipsometry in the 2–6 eV region at room temperature. Using a line shape fitting on the numerical second derivative spectra of the dielectric functions, the shifts of the E_1, E_1+Δ_1, $E_0^{'}$ and E_2 transition energies are obtained as a function of Ge composition and these are fitted as the quadratic relation between Ge compositions and transition energies. The fitting result shows that the dependences of the $E_0^{'}$ and E_2 transition energies on Ge composition are relatively weaker than that of E_1 and all transition energies show downward bowing. These behaviours of the transition edges can be interpreted as due to the shifts from valence and conduction band structure of Si to those of Ge as the Ge composition increases and due to the effect of the random potential originated by the alloying disorder.

References

[1] Kasper E and Schaffler F 1991 *Group IV compounds* in *Semiconductors and Semimetals* Vol 33 (New York: Academic) pp 223–309
[2] Soref R A 1996 *J. Vac. Sci. Technol.* A **14** 913
[3] Bean J C 1993 *Proc. IEEE* **80** 571
[4] Karunasiri R P G, Park J S and Wang K L 1991 *Appl. Phys. Lett.* **59** 2588
[5] Cohen M L and Chelikowsky J R 1998 *Electronic Structure and Optical Properties of Semiconductors* 2nd edn (Berlin: Springer)
[6] Kline J S, Pollak F H and Cardona M 1968 *Helv. Phys. Acta* **41** 968
[7] Humlicek J, Garriga M, Alonso M I and Cardona M 1989 *J. Appl. Phys.* **65** 2827
[8] Ferrieu F, Beck F and Dutartre D 1992 *Solid State Commun.* **82** 427
[9] Pickering C, Carline R T, Robbins D J, Leong W Y, Barnett S J, Pitt A D and Cullis A G 1993 *J. Appl. Phys.* **73** 239
[10] Carline R T, Pickering C, Robbins D J, Leong W Y, Pitt A D and Cullis A G 1994 *Appl. Phys. Lett.* **64** 1114
[11] Yao H, Woollam J A, Wang P J, Tejwani M J and Alterovitz S A 1993 *Appl. Surf. Sci.* **63** 52
[12] Aspnes D E and Studna A A 1975 *Appl. Opt.* **14** 220
[13] Azzam R A M and Bashara N M 1977 *Ellipsometry and Polarized Light* (Amsterdam: North-Holland)
[14] Schmid U, Humlicek J, Lukes F, Cardona M, Presting H, Kibbel H, Kasper E, Eberl K, Wegscheider W and Abstreiter G 1992 *Phys. Rev.* B **45** 6793
[15] Krist A H, Godbey D J and Green N P 1991 *Appl. Phys. Lett.* **58** 1899
[16] Lautenschlager P, Garriga M, Vina L and Cardona M 1987 *Phys. Rev.* B **36** 4821
[17] Press W H, Teukolsky S A, Vetterling W T and Flannery B P 1988 *Numerical Recipes* (Cambridge: Cambridge University Press)
[18] Junge K E, Lange R, Dolan J M, Zollner S, Dashiell M, Orner B A and Kolodzey J 1996 *Appl. Phys. Lett.* **69** 4084
[19] Kelso S M, Aspnes D E, Pollack M A and Nahory R E 1982 *Phys. Rev.* B **26** 6669
[20] Krishnamurthy S, Sher A and Chen A-B 1986 *Phys. Rev.* B **33** 1026

[21] Jones W and March N H 1973 *Theoretical Solid State Physics* Vol 2 (New York: Wiley) p 1077
[22] Bugajski M, Kontkiewicz A M and Mariette H 1983 *Phys. Rev.* B **28** 7105
[23] Kim Y D, Klein M V, Ren S F, Chang Y C, Luo H, Samarth N and Furdyna J K 1994 *Phys. Rev.* B **49** 7262
[24] Logothedis S, Cardona M and Garriga M 1991 *Phys. Rev.* B **43** 11950
[25] Lee H, Biswas D, Klein M V, Morkoc H, Aspnes D E, Choe B D, Kim J and Griffiths C O 1994 *J. Appl. Phys.* **75** 5040